Diffuse Ionized Gas in irregular galaxies: I- Gr 8 and ESO 245-G05

A.M. Hidalgo-Gámez

Instituto de Astronomía, UNAM, Ciudad Universitaria, Aptdo. 70 264, C.P. 04510, Mexico City, Mexico
and
Escuela Superior de Física y Matemáticas, IPN, U.P. Adolfo López Mateos, Mexico City, Mexico

Abstract

We have studied the spectral characteristics of the Diffuse Ionized Gas in two irregular galaxies with low metallicities and intermediate Star Formation Rates: ESO 245-G05 and Gr 8. The [OIII]/Hβ in these galaxies is higher than in the DIG of spiral galaxies but not as high as in other irregular galaxies previously studied, such as IC 10 and NGC 6822. The [NII]/Hα and [SII]/Hα ratios have very small values, indicating the absence of shocks as the ionization source for this gas. This ionization can be explained in both galaxies with photon leakage from the H II regions as the only source. The percentage of photons escaped from the H II regions is small in ESO 245-G05, of only 35%, but varies from 35% up to 60% in Gr 8. We also investigated if the differences found between spiral and irregular galaxies in the [OIII]/Hβ and the [NII]/Hα ratio are due to differences in the metal content between these types of galaxies. Although the number of galaxies studied is not very large, it can be concluded that the [OIII]/Hβ is not related with the oxygen content, while the situation is more ambiguous for the [NII]/Hα ratio.

keywords galaxies: irregular – galaxies: – interstellar medium: H II regions: general – galaxies: individual: Gr 8 – galaxies: individual: ESO 245-G05

1. Introduction

Extensive studies of the Diffuse Ionized Gas (hereafter DIG) have been carried out for spiral galaxies (e.g. Otte & Dettmar 1999). These studies show that the spectral line ratios for most of the spiral galaxies are very similar, with a very low [OIII]/Hβ, high values of [NII]/Hα, and [SII]/Hα both increasing with the distance to the plane, and high values of the ionization, as defined by [OII]/[OIII] (Tüllmann & Dettmar 2000). On the other side, the DIG properties of irregular galaxies are not known very well, as very few galaxies have been studied so far. These few data have prevented us to make any conclusion on their spectral characteristics (Martin 1997; Hidalgo-Gámez 2005; Hidalgo-Gámez & Peimbert 2006). These data show that the line ratios differ from those in spiral galaxies. The [OIII]/Hβ is large. For some of the galaxies, e.g. IC 10, is larger than 1.5. The [NII]/Hα and [SII]/Hα ratios are smaller than 0.5. Moreover, if the line ratios are very different for spiral and irregular galaxies, it is likely that the ionization source of the DIG will also differ due to different metal contents, gas masses or Star Formation Rates (SFR).

In the present investigation we study two dwarf irregular galaxies with low chemical abundances and intermediate SFRs: Gr 8 and ESO 245-G05. The first one is a nearby galaxy at a distance of D = 2.24 Mpc (Hidalgo-Gámez & Olofsson 1998) dominated in the optical by two large H II regions. The metallicity is very low (12+log(O/H) = 7.4±0.1, Hidalgo-Gámez & Olofsson 2002) and also the SFR, which is 2.12×10^{-3} $M_\odot$ yr^{-1} (Hunter & Elmegreen 2004). ESO 245-G05 is one of the Sculptor group dwarf galaxies. The oxygen content is also low (7.6-7.8 with small variations along the bar, see Hidalgo-Gámez et al. 2001) and the SFR is 1.1×10^{-2} $M_\odot$ yr^{-1} (Miller 1996). In both galaxies, a large extension of ionized gas in their Hα images is present. Therefore, they represent good candidates for studying the properties of the DIG. Due to their low metallicities they could be used to study the dependence of the DIG properties with some of the characteristics of the irregular galaxies.

The paper is structured as follows: the observations and the reduction of the data are described in the next Section. In Section 3, the line ratios along the slit for each galaxy are presented. Possible sources of ionization of the Diffuse Gas are described in Section 4. Section 5 discusses the relation between the metallicity and the DIG properties. Conclusions are presented in Section 6.

2. Observations and data reduction

The data were obtained with two different facilities. The spectrum of ESO 245-G05 was acquired on August 9th, 1997 with the 3.6m telescope at La Silla Observatory with EFOSC1. All the details about the data acquisition and the reduction procedure are described in Hidalgo-Gámez et al. (2001) and, therefore, are not going to be repeated here. We will remember that the slit position used for this analysis had a position angle of 295 degrees, covering the southern part of the bar (see Figure **??**), and the real spectral resolution was 18Å. These data were acquired and reduced without considering the low surface brightness emission and, therefore, the sky subtraction was severe in order to eliminate the strongest sky lines.

The spectra of Gr 8 were obtained on March 13th-14th, 2002 with the 2.1-m telescope of the Observatorio Astronómico Nacional at San Pedro Mártir (OAN-SPM). The Boller & Chivens spectrograph was used with a 300 l/mm grating blazed at 5000 Å. The slit width was 170 μm, subtending $\approx 2''$ on the sky, and yielding a spectral resolution of 7 Å. The full spectral range observed was 3500-6900Å. The first night (13/03/02) was not very photometric, due to cirrus and strong wind, whereas during the second night weather conditions were good, although the seeing was high. Table 1 shows the log of observations. No correction for differential refraction was performed as the pixel size was small and also the airmasses were smaller than 1.3 in all the slit positions but one. The orientation of the slits was E-W with a total of six slit positions.

The reduction of the Gr 8 data was performed with the MIDAS software package. Bias and sky twilight flatfields were used for the calibration of the CCD response. Due to the strong differences in the sensitivity of the CCD as to the wavelength, the spectral range was divided into three parts: from 5200 Å to 6800 Å (red), from 4000 Å to 5600 Å (green) and from 3500 Å to 4800 Å (blue). Unfortunately, due to the low efficiency of the spectrograph at the blue end, no spectral lines were detected there and, therefore, they were not used in the present investigation. He-Ar lamps were used for the wavelength calibration. The spectra were corrected for atmosferic extinction using the San Pedro Mártir tables (Schuster & Parrao 2001). Several standard stars were observed each night in order to perform the flux calibration. The accuracy of the calibration was better than 5% for both nights. The most difficult task was the sky subtraction because removing the strong sky lines of the spectra will also remove most of the low surface brightness emission. Therefore, only a dozen of rows were used in the sky templates for each spectrum and only the underlying sky structure was subtracted, but most of the stronger sky lines still remain in the spectra. Special care was taken in the analysis procedure for these data. However, it will not affect the results because a strong sky subtraction was perfomed on the ESO 245-G05 data, being the results very similar (see Section 3).

Both sets of data, fully reduced and calibrated, were divided into a number of spectra, covering three rows for ESO 245-G05 and five for Gr 8 (hereafter, the r-spectra). The total sizes are 1.8 and 5 arcsec, respectively. These values match the seeing conditions and corresponds to 39 pc in ESO 245-G05 and 40 pc in Gr 8. The total number of spectra studied was 51 for the slit position of ESO 245-G05 and 77 for the six positions in Gr 8.

Finally, we wish to comment on the uncertainties. Three different sources were considered: the uncertainties in the level of the stellar continuum with respect to the line, σ_c, those introduced by the reduction procedure, σ_r, (especially flatfielding and flux calibrations) and uncertainties due to the extinction correction, σ_e. The final uncertainty for each line was determined from

$$\sigma = \sqrt{\sigma_c^2 + \sigma_r^2 + \sigma_e^2}$$

These uncertainties were measured for each line at each spectrum in all the positions for each galaxy. With these values a total uncertainty for each line and each slit position can be determined, and is presented in Table 2.

3. Diffuse Ionized Gas

As previously said, the main purpose of this investigation is to obtain the spectral characteristics of the Diffuse Gas in the mentioned irregular galaxies. Spiral galaxies are the main targets in DIG studies, mainly because the DIG is situated above the plane of the disk (e.g. Otter & Dettmar 1999) or in the inter-arm region (Benvenuti et a. 1976). In the case of the Milky Way, the low density is the main characteristic for the discrimination.

The difficulties of studying DIG in irregular galaxies are due to the problem of distiguishing between the ionized gas inside and outside the borders of the classical the H II regions. A disk is not clearly defined in these galaxies. Moreover, density is one of the most difficult parameter to determine from long-slit spectroscopy data. The only way to do so is by using the ratio of the lines of any of the following doublest: [OII]$\lambda\lambda$3726,3729Å, [SII]$\lambda\lambda$6717,6731Å, [ClIII]$\lambda\lambda$5517,5537Å and [ArIV]$\lambda\lambda$4711,4740Å (Aller 1984). Therefore, any of these doublets should be detected and resolved with high accuracy. The one mostly used is [SII]λ6717/[SII]λ6731 because the intensity of the lines is high enough to be detected, and not very high spectral resolution is needed. The main drawback is that in the low density regime the differences in the [SII]λ6717/[SII]λ6731 between the H II regions, with typical densities of 100 cm^{-3}, and the DIG with values of 10 cm^{-3}, are about 0.1 (see figure 5.3 in Osterbrock 1989), which normally is smaller than the uncertainties in the ratio. The situation is even worse for the other doublets. Thus, the density cannot be used for the discrimination of the DIG and the H II regions.

Another parameter involved in the definition of the DIG is the Emission Measure (EM) related to surface brightness (SB) in Hα and the electronic temperature (Greenawalt et al. 1998). In the Milky Way there is a correlation between low EM and low density. Therefore, the EM can be used in the discrimination between DIG and H II regions when the density cannot be determined. The main difficulty is the lack of an unique value for the EM. It varies from 80 pc cm^{-6} for the arms in spiral galaxies (Hoopes & Walterbos 2003) to 2 pc cm^{-6} for the Milky Way (Reynolds 1989). Instead of choosing a value in this range, we decided to use another approach. The cumulative distribution function of the surface brightness in Hα is a smoothly increasing function with a change in the slope when H II regions begin to dominate the light. This SB(Hα) turnoff point can be considered as the discriminator between DIG and H II regions. This procedure has already been used for the two previous galaxies studied by the author (IC 10, Hidalgo-Gámez 2005; NGC 6822, Hidalgo-Gámez & Peimbert 2006). It has to be kept in mind that this procedure, as any statistical method, is more accurate for a large number of data points especially when are included both cores of the H II regions and very weak emission regions.

Figure 1 shows this function for Gr 8 and ESO 245-G05. Both galaxies have a turn-off point of log SB(Hα) $\approx$ -17.9, which corresponds to 1.3×10^{-18} erg cm^{-2} s^{-1} arcsec^{-2}. The surface brightnesses have been corrected for Galactic extinction following Schelgel et al. (1998). Another turn-off point is detected, especially in ESO 245-G05 at 2×10^{-19} erg cm^{-2} s^{-1} arcsec^{-2}, which might be an indication of the noise level. There are only two data points with SB(Hα) lower than this limit and they are not going to be considered hereafter. Therefore, we will regard as DIG data those spectra with SB(Hα) between 2 and 13 10^{-19} erg cm^{-2} s^{-1} arcsec^{-2}. The latter value is slightly lower than in the other two irregular galaxies studied by the author, which gives log SB(Hα) = $-$17.45 for NGC 6822 (Hidalgo-Gámez & Peimbert 2006) and log SB(Hα) = $-$17.5 for IC 10 (Hidalgo-Gámez 2005), both galaxies having larger SFRs and metallicities. This range splits the spectra into 21 H II regions and 56 DIG locations in Gr 8. The corresponding values in ESO 245-G05 are 20 and 29, respectively. In addition, two points with surface brightness on the boundary between the DIG and the H II locations were found in this last galaxy.

In order to test the correctness of this cumulative function for defining H II regions we can study the relation between the SB(Hα) and the line ratios. Fig 2 shows the log SB(Hα) vs. [SII]/Hα for ESO

245-G05 (a) and Gr 8 (b) for all the data points of the r-spectra. There is a trend toward having lower [SII]/Hα for larger SB, especially for Gr 8 while there is a turn-off point at log SB(Hα) = - 18.1 for ESO 245-G05. There is also a bifurcation for the H II regions which could be related with diferences in the chemical content (Martin 1997). An opposite trend is shown in Figure 3 between log SB(Hα) vs. log [OIII]/Hβ for both galaxies. The smooth transition between DIG locations and H II regions indicates that the distinction between them is correct. Another way to verify it is to compare the size of the H II regions determined from the cumulative function and the extension of the spectral lines. The sizes obtained with the cumulative function correspond to the high ionization regions. Therefore, although the cumulative function is a statistical approach, it serves as a good distinction between DIG and H II regions when density cannot be determined.

In addition to the r-spectra defined in the previous section, the so-called integrated spectra were obtained summing up all the pixels with surface brightness lower than 1.3×10^{-18} erg cm^{-2} s^{-1} arcsec^{-2} (DIG) and higher than it (H II) to obtain spectra of high S/N for each H II and DIG region.

In the following, we will study the variations along the slits of the line ratios of interest for each galaxy.

3.1. ESO 245-G05

As already said, there is only one slit position for this galaxy. In both the r-spectra and the integrated ones, the recombination lines Hα, Hβ, as well as the forbidden ones [OII]λ3727Å, [OIII]λ5007Å, [NII]λ6583Å, [SII]λ6717Å and [SII]λ6731Å, were determined. The hidrogen line Hγ was detected at very few locations, mainly corresponding to H II regions. The intensities of all the lines were normalized to Hβ, and the ratios [OII]λ3727/Hβ, [OIII]λ5007/Hβ, [NII]λ6583/Hα, [SII]λ6717/Hα and [SII]λ6717/[SII]/λ6731 were obtained. The reddening correction is very important when comparing intensities of lines with very different wavelengths. Unfortunately, the ratio Hα/Hβ cannot be used for the extinction determination, as explained in Hidalgo-Gámez et al. (2001). In that investigation the Hγ/Hβ was used for the reddening correction. But, as previously said, the Hγ line was not detected elsewhere and therefore, it was not a solution here. In consequence, no reddening correction was performed. For the majority of the line ratios the wavelength range is very narrow and the values remain, essentially, unaffected. The only exception is the [OII]/Hβ ratio where the differences between the non-corrected and the corrected values might reach up to 30%. Therefore, we are not going to discuss this ratio here. Table 3 shows the line ratios from the integrated spectra with a total of 3 H II regions and 4 DIG regions. Due to the smaller width of the slit and the high resolution of this configuration, the ratio [SII]λ6717/[SII]λ6731 is quite reliable. The number of pixels of region *d1* is very small and so is the S/N. Therefore, it is not useful for obtaining any conclusion.

The line ratios along the slit for the surface brightness, the excitation the [SII]/Hα and the density are shown in figures from 4 to 7. The H II regions are marked by dashed-dotted lines while the values from the integrated spectra are shown by dashed lines. Fig. 4 shows the SB(Hα) along the slit. The most interesting feature is that *h3* is formed by two condensations, with a region of low surface brightness between them. As there was only one data-point, it was considered a transition point and part of the H II region. Moreover, the second condensation has the large SB in the region under study.

The excitation, defined as [OIII]λ5007/Hβ, is larger inside H II regions (Fig. 5), being the only exception the spectra No *61-63*, where the [OIII]/Hβ is larger than in *h2*. This is not considered anomalous as these fluctuations are observed in other galaxies too (e.g. IC 10, Hidalgo-Gámez 2005). It is very interesting that the [OIII]λ5007Å line was not detected either the majority of *d2* spectra or in the integrated spectra, which is an indication of very few [OIII]/Hβ of the DIG in this region. Other interesting feature is the very low [OIII]/Hβ, dropping to 0 at the transition point in the eastern condensation of *h3*.

The second interesting line ratio is [SII]λ6717/Hα which is shown in figure 6. From Table 2 it could be seen that the values of this ratio increase along the slit towards the west for H II, while it is almost constant for DIG locations. The very large values of this ratio inside the H II regions are very disturbing. Such values are very unusual as normally, this ratio is very low inside H II regions, lower than 0.05 (Hidalgo-Gámez & Olofsson 2002), but it reaches up to 0.47 inside *h3*. This high value coincides with the first condensation of this region while the transition point has a value of 0.27. In the case of the other two H II regions, the values (both integrated and along the slit) are very similar to what is obtained for other irregular galaxies (e.g. Hidalgo-Gámez & Peimbert 2006). As far as the DIG locations concern, there are two peaks of 0.41 and 0.29 at both ends of *d2*, but the averaged values are very similar to those in Gr 8 (see Section 3.2). As it is well known, for values larger than 0.3, shocks might be important contributors to the ionization of the lines (Dopita 1993). Except for these three spectra (No *41*, *52* and *66*), the values indicate that shocks are not important elsewhere.

Finally, we can discuss the ratio [SII]λ6717/[SII]λ6731, which is related with the density (Osterbrock 1989). DIG locations have smaller density and, therefore, larger [SII]/[SII] ratios. From Table 3 we see that all the regions, except maybe *h1* and *d2*, are inside the low density limit. The exact value of the density cannot be determined, as previously discussed. Moreover, some of the values are above the theoretical limits due to the blending of the lines, which is an indication of very low densities.

3.2. Gr 8

A similar procedure was used for Gr 8. Because of the low efficiency of the B&Ch spectrograph at the blue end, [OII]λ3727Å was not detected. The lines Hα, Hβ, [OIII]λ5007Å, [NII]λ6583Å, [SII]λ,λ6717,6731Å were measured in the r-spectra. Due to the spectral resolution of this configuration, the two lines of [SII] cannot be resolved properly and we prefered to have only a measured of both lines together. Their intensities were normalized to Hβ and extinction corrected using the Hα/Hβ ratio. Because the line [NII]λ6583Å was detected in only a few locations along each slit position, it is not interesting to study its variations along the slits. In fact, it was detected in only one DIG integrated spectrum. Thus it was not a configuration problem but a real deficiency of nitrogen in this galaxy. Moreover, Fabry-Perot interferometry indicates that nitrogen is located at a very small part of the western H II region (M. Rosado, private communication). In addition, the recombination line He I λ5876Å was detected in four H II regions of the integrated spectra. Therefore, the ratios of interest in Gr 8 are only [OIII]λ5007/Hβ and [SII]$\lambda\lambda$6716,6730Å/Hα. Besides these, the surface brightness and the extinction along each slit can also be studied.

In Table 4 the surface brightness, the [OIII]/Hβ and the [SII]/Hα ratios are given for all the integrated spectra, as well as the extinction coefficient. The values of [NII]λ6584Å and HeIλ5876Å are also tabulated when detected.

Figure 8 shows the surface brightness in Hα along the slits for each of the six slit positions. The x-axis corresponds to the number of the spectra. The orientation is from the north of the galaxy in the upper part of the figure (slit f) to the south at the bottom (slit a). The H II regions are marked between dash-dotted lines. As seen in Table 1, the distance between the slit positions is not the same for all of them. Therefore the H II regions are not coincident. In any case, it is interesting to notice the movement of the emission from west (at the left) to east (at the right). Also, the H II regions move in the same direction. This displacement is not due to the movement of the galaxy on the sky which would give a displacement in the opposite direction but to the orientation of the galaxy, which is south-west to north-east, as observed in this Figure. Finally, the sizes of the H II regions vary from only 37 pc to 200 pc, fitting the orientation of the galaxy. With this information we can identify the H II regions with the most prominent regions named nr 5 in slits *a)* and *b)* and nr 19 in the

rest of the positions of Hodge et al. (1989).

Figure 9 shows the [OIII]/Hβ. The orientation is the same as in Figure 8. In addition to the H II region positions, the values of the integrated spectra as shown in Table 4 are given by the dotted lines. All the slit positions have the same range in [OIII]/Hβ in order to see their differences throughtout the galaxy. In this sense, slits (a) and (b) have the largest [OIII]/Hβ ratio, while it decreases towards the north, reaching a minimun at slit (f). Considering the [OIII]/Hβ throughout each slit position, the H II regions have, in general, the largest [OIII]/Hβ, but there are exceptions. In fact, there is not a general guideline. For example, the values of the [OIII]/Hβ are very different in H II and DIG locations for slit *(a)*, while they are of the same order in slits *(e)* and *(f)*. In the case of slits *(c)* and *(d)* the [OIII]/Hβ of the DIG is larger towards the west than towards the east. This agrees with the surface brightness distribution of Hodge et al. (1989). For all the positions, there is a good agreement between the values for the integrated spectra and the r-spectra. Indeed, the largest values of the integrated spectra correspond to *bh1* and *ah*, which are also the locations with the largest [OIII]/Hβs in the r-spectra. Another important fact to be noticed is that, contrary to the previous irregular galaxies study by the author (IC 10 and NGC 6822), there are DIG locations with very low [OIII]/Hβ, lower than 0.5, such as *cd2* and *dd2*.

Figure 10 shows the [SII]/Hα ratio. The orientation and the meaning of the lines as in Fig. 8. The range in all the slits is the same, between 0 and 1. The highest value of this ratio is in slit *b)*, with [SII]/Hα = 1, but only in slits *f* and *d* some locations have values larger than 0.3. The value of spectrum *bd1* is very striking because although the Hα images of this galaxy reveal two large H II regions (Hodge 1967) with star forming activity, the Star Formation Rate is low, only 2.2×10^{-3} $M_\odot$ yr^{-1} (Hunter & Elmegreen 2004). Moreover, there are no superbubbles reported in this galaxy which might explain the large values of the [SII]/Hα ratio. Begum & Chengalur (2003) interpreted their results in H I for this galaxy as a combination of rotation and a radial movement (expansion outwards because of the star formation activity or infall inwards due to the formation process which has not been completed yet). But in their maps, there is no particular disturbance at the locations of spectra *bd1* or *dd2*. In any case, the results of Fig. 10 are in agreement with those from Fabry-Perot interferometry of this galaxy (Rosado, private communication). In general, the values of [SII]/Hα are smaller inside H II regions than in DIG locations. However, there are a few places where these differences are very small, as occurs in *bd2*. Once again, the agreement between the integrated and the r-spectra is very good, in general.

Begum & Chengalur (2003) also noticed that the H I is clumpy, and they considered it is associated with the optical emission. A similar conclusion can be reached from Figure 11, showing the extinction coefficient along the slits. From this figure, a very interesting result can be inferred. The concentration of dust is not homogenous along the slits and does not follow any pattern. The largest C_β values of some of the slits are inside the H II regions (slit *(d)*) while in other cases, such as slit *(e)*, the maximun value of the C_β is found at a DIG location. Apparently, these results do not agree with those from Begum & Chengalur (2003). A possible explanation is that their large observing resolution prevent them from observing the interior of the H II regions, as we have done here. In fact, there is a good agreement between both investigations, as the extinction values are very large in all but one position (*bd1*).

The spectral characteristics of the emission lines in ESO 245-G05 are very different from what is observed in other galaxies, not only at the DIG locations but also at the H II regions, due to the very large values of [NII]/Hα and [SII]/Hα. The situation in Gr 8 is more similar to what is found in other galaxies. In the following, we are going to find the model which fits best all the line ratios in both galaxies.

4. The ionization source

4.1. Radiation bounded vs. density bounded H II regions

The theory of H II regions was developed by Strömgren in 1939 and since then they have been considered as radiation bounded (Aller 1984). In this case, there is not enough nearby neutral gas to absorb the total Lyman continuum of the source and form a classical Strömgrem sphere. With such a model the line ratios can be predicted when the ionizing temperature of the OB associations is known (Osterbrock 1989). This is true not only for the region inside the Strömgren radius (the classical H II region) but also for the gas outside this limit, the Diffuse Ionized Gas. Mathis (1986) and Domgörgen & Mathis (1994) made preditions on the line ratios of the DIG for different ionization parameters. They concluded that both [NII]/Hα and [SII]/Hα are larger than 0.3 and the [OIII]/Hβ is very low (< 0.1). Another important result is the constancy of the [NII]/Hα ratio between the DIG and the H II regions (Mathis 1986), as well as a lack of correlation between this ratio and [SII]/Hα. In recent years it has been considered that H II regions may be density instead of radiation bounded (Beckman et al. 2000). It would means that photons still would have enough energy to ionize the gas outside the classical Strömgren sphere. Moreover, considering inhomogeneities in the density inside the H II region (Giammanco et al. 2004), the escape of photons is not the same in all directions. Using such a model, Hoppes & Walterboos (2003) predicted the line ratios of the DIG for an Orion metallicity and an ionization parameter of 10^3.

We can compare the data in Tables 3 and 4 with the predictions of both models by taking into account that they both were made for higher metallicity regions than those considered here. A lower metallicity implies a high ionization parameter, which implies higher [OIII]/Hβ. Moreover, a consequence of the leakage of photons is a harder spectrum, therefore higher [OIII]/Hβ for the same T_{ion}.

Classical photoionization theory (radiation bounded) cannot explain the line ratios of these galaxies. The main reasons are that even though the [OIII]/Hβ is lower in these two galaxies than in other irregular galaxies, it is not as low as 0.1 in any place, and only lower than 0.4 in *cd2* and *dd2* in Gr 8 and in *d1* in ESO 245-G05. Also, neither [NII]/Hα nor [SII]/Hα show very large values but only in those spectra discussed in sect. 3. There is no improvement either when lower metallicities are considered (see Hidalgo-Gámez & Peimbert 2005 and references therein).

Another argument is found in Figure 12 which shows the log [NII]/Hα vs. log [SII]/Hα for ESO 245-G05 and Gr 8. The symbols are the same for both galaxies: diamonds stand for H II regions, stars for DIG and, in the case of ESO 245-G05, the two transition points are represented by triangles. These two parameters show a correlation for the DIG in spiral galaxies which cannot be explained by photoionization (e.g. Rand 1998). Recently, Wood & Mathis (2004) reproduced such correlation using Montecarlo simulations with photoionization models. They explained this correlation by the temperature increase away from the ionizing sources with the increasing distance from the plane. There is a correlation in Figure 12 between H II regions of ESO 245-G05, while a scatter diagram is given for DIG locations of this galaxy and for all the data points of Gr 8. This figure cannot be explained by any change in the Wood & Mathis's models. In irregular galaxies the ionizing sources are located in all directions and therefore there are no important changes in the temperature. Another explanation might be variations in the abundances of nitrogen or sulfur. Irregular galaxies are considered as chemicaly homogeneous galaxies and only NGC 5253 shows a local enhancement of nitrogen, probably due to the WR population (Kobulnicky et al. 1997). Nothing can be said about the nitrogen distribution in ESO 245-G05 because it was measured in only one H II region. Considering Gr 8, Moles et al. (1990) reported differences in the log N/O of 0.28 while only 0.03 in log O/H between two H II regions. If these are real nitrogen variations they can explain the lack of correlation observed in Figure 12.

We are going to check if photon leakage models (density bounded regions) can explain better the

intensities of the line ratios observed. The study of ESO 245-G05 is easier because there are only four DIG regions (see Table 2). For all of them, both the T_{ion} and the percentage of photon leakage agree when all the line ratios are considered. Values of 40% from the [OIII]/Hβ, 30% from the [NII]/Hα, and between 35 to 80% from [SII]/Hα are obtained. The T_{ion} is between 35,000 K and 40,000 K in all the cases. Considering the low metallicity of this galaxy, a leakage of photons of 35% and an ionization temperature of 40,000 K can account for all the three line ratios.

The study of the DIG in Gr 8 is more difficult, not only because of the large number of locations but also due to the wide range in temperatures and leakages. Moreover, the nitrogen ratio was detected only in one DIG location and therefore only the [OIII]/Hβ and the [SII]/Hα are used. Table 5 shows the percentage of leakage and the T_{ion} from the two ratios. To explain the [OIII]/Hβ, a leakage of at least 50% is needed, while the [SII]/Hα gives values no larger than 40%. Surprisingly, both ratios give similar temperatures of $\approx$ 35,000-40,000 K. Considering that the metallicity of this galaxy is extremely low, 12+log(O/H) = 7.4$\pm$0.1 (Hidalgo-Gámez & Olofsson 2002), metallicity can be regarded as the reason for the high values of the [OIII]/Hβ.

A quick inspection of Table 5 shows that the leakage needed from the [OIII]/Hβ if lower abundances are considered, is still much larger than the leakage from the sulfur ratio ($\approx$ 35 %). One explanation could be that the emission from these two lines originates in two different regions. In order to produce [OIII]λ5007Å, very energetic photons are needed. Therefore, the regions where this line originates must be closer to the H II regions with T_{ion} larger than 40,000 K, while the [SII]λ6717Å might be originated futher away from the H II regions and, therefore, the temperature is lower and the photons softer. Moreover, as we said before, the slits covered a large part of the galaxy and therefore, conditions can vary for each slit position. For example, slits *(a)*, *(b)* and *(f)* might have a large leakage, of 50% or even larger for slit *(b)*, in the [OIII] region. The slits *(c)* and *(d)* are the most problematic to explain because the only values of T_{ion} and leakage from [OIII]/Hβ are very different from the range obtained from the [SII]/Hα ratio.

Therefore, in order to explain the ionization of the Diffuse Gas in Gr 8, not a single value of the leakage of photons but several of them should be used, because physical conditions (density, ionization temperature, etc) vary along the galaxy.

4.2. An extra ionizing source from shocks or turbulence?

We can use the models from Dopita & Sutherland (1995) to study the contribution of shocks to the ionization of the DIG. From their table 1 it can be obtained that the [SII]/Hα ratio is larger than 0.18 for a model of shock+precursor with a shock velocity of 200 km s^{-1}. Regions *d2*, *d3* and *h3* in ESO 245-G05 marginally reach this value whereas it is higher for regions *ad1*, *bd1*, *ed1* and *fd1* in Gr 8. The main objection is that the [OIII]/Hβ is very high ($\approx$ 1.6) when this shock velocity is considered and none of these regions have such values. Three of them have [OIII]/Hβ smaller than 1.

Another important tool in the study of shocks are the diagnostic diagrams. Figure 13 shows the log[OIII]/Hβ vs. log[SII]/Hα diagram for both galaxies. The solid line divides the diagram into the photoionization (to the left) and the shocks (to the right) regions from Veilleux & Osterbrock (1987). Only two data points lie in the shocks region for ESO 245-G05, and none of them are DIG locations. In contrast, a few of DIG spectra in Gr 8 lie very close to the border line. These results are in agreement with those obtained in the previous paragraph, where very few locations might reach the values in the [SII]/Hα ratio that would indicate shocks. In both cases we might expect that shocks play a more important role in these galaxies. The lack of detectable shock waves is interesting because the velocity field of ESO 245-G05 is very peculiar maybe because of past interactions (Cote et al. 2000). A possible explanation is that only one slit position at the southern end of the galaxy is studied here. Gr 8 is kinematically supported by random motions (Begum & Chengalur

2003) and a total of 6 slit position, covering the most of the optical body of the galaxy have been studied. Therefore, it can be concluded that the gas motions inside Gr 8 are not very strong and do not have important consequences in the ISM.

Another interesting feature is the trend observed for ESO 245-G05, where the higher the [OIII]/Hβ, the lower the [SII]/Hα is, with the DIG locations at the lower end of the trend. On the contrary, the segregation in Gr 8 is more horizontal, with the DIG locations generally closer to the shock line than the H II regions.

Finally, we can discuss another interesting model related to shocks as is the so-called Turbulent Mixing Layer by Slavin et al. (1993). This model contemplates the existence of a turbulent layer as the ionization source of the DIG. Slavin et al. predicted the line ratios with the transverse velocity of the hot gas (v_t), the intermediate temperature after mixing (T^-) and the abundance. When comparing here the values in Tables 3 and 4 with their figure 5 it is clear that [NII]/Hα cannot be fitted with any set of parameters, whereas the [OIII]/Hβ and [SII]/Hα require differences in the T^- of a factor of 2, from 10^5 to 2×10^5 K. This last result is not surprising as this model is optimized for low ionization ions (Slavin et al. 1993)

From this discussion we therefore conclude that no clear indication exists about an extra ionization source of the DIG in these galaxies.

5. Discussion

When comparing the DIG line ratios of spiral galaxies (Otte & Dettmar 1999) with those in irregular galaxies there appear two very striking characteristics: the higher [OIII]/Hβ and the lower [NII]/Hα ratio in irregulars compared to spirals. It is possible that the main reason for such a difference is the different metal content between these two type of galaxies. Irregular galaxies have metallicities in the range of 1/15-1/30 $Z_\odot$ (e.g. Hidalgo-Gámez & Olofsson 2002). One might think that as there are less metals, the intensity of the lines is lower and, therefore, the ratios are also lower. This is true for nitrogen but there is an anticorrelation between the content of oxygen and the electronic temperature (and, therefore, the [OIII]/Hβ) as oxygen is a very powerful coolant (e.g. Alloin et al. 1979).

In order to check if the anomalous values of these two ratios in irregular galaxies are due to low metallicity of the parent galaxies, we plot the [OIII]/Hβ vs. the oxygen content (Fig. 15a) and the [NII]/Hα vs. the nitrogen abundances (Fig. 15b) for a sample of irregular galaxies: IC 10 (Hidalgo-Gámez 2005), NGC 6822 (Hidalgo-Gámez & Peimbert 2005), DDO 53 (Hidalgo-Gámez & Flores-Fajardo, in preparation), DDO50, IC 5152 (Hidalgo-Gámez, in preparation) and ESO 245-G05 and Gr 8 (this work). Only five of them have reliable nitrogen abundances and [NII]/Hα ratios. Three out of the five galaxies lie in the same line, with IC 5152 very far from this relationship. Gr 8 has a very low nitrogen abundance (12+log(N/H) = 5.4; Moles et al. 1990) but the [NII]/Hα ratio, detected at only one DIG location, is very high. On the contrary, DDO 53 has higher nitrogen abundance, 7.7, but the line [NII]λ6583Å was not detected at any DIG location. More data are needed to confirm the relationship between the nitrogen content and the [NII]/Hα ratio.

Considering the [OIII]/Hβ, an inverse anticorrelation is expected because oxygen is an important coolant of the ISM. Then, the lower the oxygen content, the higher the electronic temperature is, to which the intensity of the [OIII]λ5007Å line is related. The trend shown in Figure 15a is a correlation between the [OIII]/Hβ and the oxygen content. Two of the galaxies with the higher metallicities have very large [OIII]/Hβ, while those with smaller oxygen content have significantly lower [OIII]/Hβ. The most discordant galaxy is IC 5152, probably because the metal content and the DIG line ratios were measured in very different parts of the galaxy: the outskirts and the very center of the galaxy, respectively. Therefore, the differences in the value of the [OIII]/Hβ between spiral and irregular galaxies are real and not due to the different metal content.

6. Conclusions

In the present investigation we have studied the spectral characteristics of the Diffuse Ionized Gas in two irregular galaxies. In the other two irregular galaxies previously studied by the author it was found that the [OIII]/Hβ was much higher than in the DIG of spirals. One of the reason argued was the low metallicity of the irregular galaxies (D. Cox, private communication). In order to study if this was real, we chose two galaxies with very low metallicity and intermediate Star Formation Rate.

We have studied the [OIII]/Hβ, the [NII]/Hα and the [SII]/Hα ratios along one slit position in ESO 245-G05. These last two ratios exhibit strange behaviour at the DIG locations. The main source of ionization of the DIG is photon leakage from the H II regions. A similar study has been done for a total of six slit positions at Gr 8. Although some of the DIG data points have very large values of the [SII]/Hα ratio which might indicate the presence of shocks, the main ionization source is, again, photon leakage with values between 40% and 75%.

Finally, we studied the relationship between the [OIII]/Hβ and the oxygen content. If, as proposed, the low metallicity is the reason for the higher [OIII]/Hβ, an anticorrelation is expected between these two parameters. Although there are only data for seven galaxies the opposite trend is obtained, and therefore it can be concluded that the high [OIII]/Hβ is not due to low metallicity.

The author is indebted to many colleages at IA-UNAM for many useful comments on this work. An anonymous referee is thanked for helpful and interesting comments and discussion which have improved this manuscript. She also thanks to F.J. Sánchez-Salcedo for a carefully reading of the manuscript. This investigation is partly supported by CONACyT project 2002-c40366.

REFERENCES

Aller, L.H. 1984, Physics of Thermal Gaseous Nebulae, D. Reidel Publishing Company, Dordrecht

Alloin,D., Collin-Souffrin, S., Joly, M & Vigroux, L. 1979, A&A, 78, 200

Beckman, J.E., Rozas, M.T., Zurita, A., Watson, R.A., & Knapen, J.H. 2000, AJ, 119, 2728

Begum, A., & Chengalur, J.N. 2003, A&A, 409, 879

Benvenuti, P., D'Odorico, S., & Peimbert, M. 1976, RevMexA&A, 2, 3

Cote, S., Carignan, C., & Freeman, K.C. 2000, AJ, 120, 3027

Domgörgen, H., & Mathis, J.S. 1994, ApJ, 428, 647

Dopita, M.A. 1993, PASAu, 10, 359

Dopita, M.A., & Sutherland, R. 1995, ApJ, 455, 468

Greenawalt, B., Walterbos, R.A.M., Thilker, D.,& Hoopes, G.C. 1998, ApJ, 506, 135

Giammanco, C., Beckman, J.E., Zurita, A., & Relaño, M. 2004, A&A, 424, 877

Hidalgo-Gámez, A.M., & Olofsson, K. 1998, A&A, 334, 45

Hidalgo-Gámez, A.M., Masegosa, J., & Olofsson, K. 2001, A&A, 369, 797

Hidalgo-Gámez, A.M. & Olofsson, K. 2002, A&A, 389, 836

Hidalgo-Gámez, A.M. 2005, A&A, 442, 443

Hidalgo-Gámez, A.M. & Peimbert, A. 2006, in preparation

Hodge, P.W. 1967, ApJ, 148, 719

Hodge, P.W., Lee, M.G., & Kennicutt, R.C., Jr. 1989, PASP, 101, 640

Hoopes, G.C., & Walterbos, R.A.M. 2003, ApJ, 586, 902

Hunter, D.A., & Elmegreen, B.G. 2004, AJ, 128, 2170

Kobulnicky, H.A., Skillman, E.D., Roy, J-R. Walsh, J.R., & Rosa, M.R. 1997, ApJ, 477, 679

Martin, C.L. 1997, ApJ, 491, 561

Mathis, J.S. 1986, ApJ, 301, 423

Miller, B.W. 1996, AJ, 112, 991

Moles, M., Aparicio, A., & Masegosa, J. 1990, A&A, 228, 310

Otte, B., & Dettmar, R-J. 1999, A&A, 343, 705

Osterbrock, D.E. 1989, Astrophysics of Gaseous Nebulae and Active Galactic Nuclei, University Science Books, Mill Valley, CA

Rand, R.J. 1998, ApJ, 501, 137

Reynolds, R.J. 1989, ApJ, 345, 811

Schlegel, D.J., Finkbainer, D.P., & Davis, M. 1998, ApJ, 500, 525

Schuster, W.J., & Parrao, L. 2001, RevMexA&A, 37, 187

Slavin, J.D., Shull, J.M., & Begelman, M.C. 1993, ApJ, 407, 83

Strömgren, B. 1939, ApJ, 89, 526

Tüllman, R., & Dettmar, J-R. 2000, A&A, 362, 119

Veilleux, S., & Osterbrock, D.E. 1987, ApJS, 63, 295

Wood, K., & Mathis, J.S. 2004, MNRAS, 353, 1126

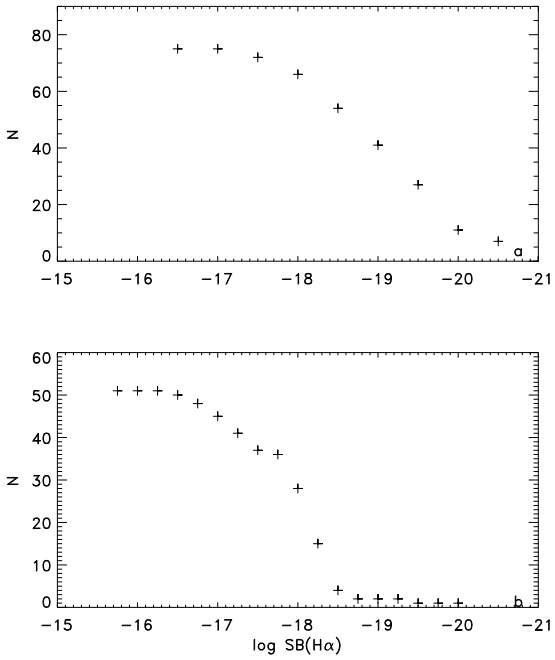

Fig. 1.— The cumulative distribution function of the surface brightness in Hα, Galactic extinction corrected, for Gr 8 (panel a) and ESO 245-G05 (panel b). Both galaxies show a turn-off point at log SB(Hα) = -17.9, indicating the transition between DIG and H II regions.

This preprint was prepared with the AAS LaTeX macros v5.2.

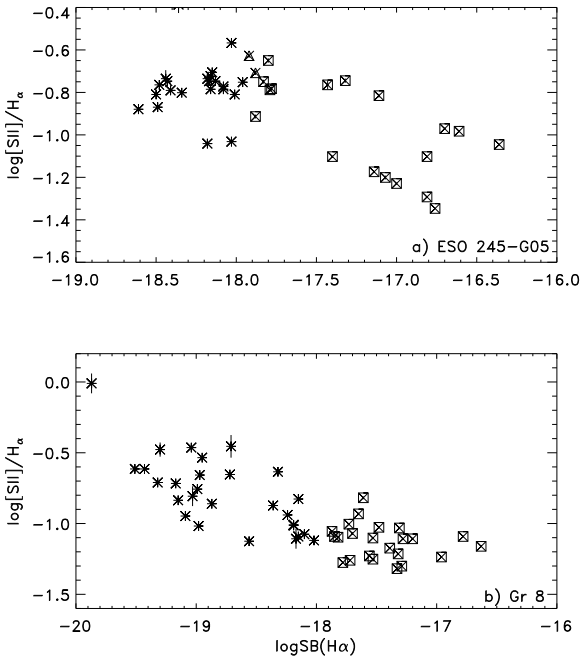

Fig. 2.— The log SB(Hα) vs. [SII]/Hα for Gr 8 (panel b) and ESO 245-G05 (panel a). DIG locations are plotted as stars and H II as squares. The two transition points in ESO 245-G05 are plotted as triangles (see text for a definition). The error bars associated with every data fromt he r-spectra are presented. The data points shows an anticorrelation for Gr 8 while the DIG data points exhibit a scatter diagram for ESO 245-G05.

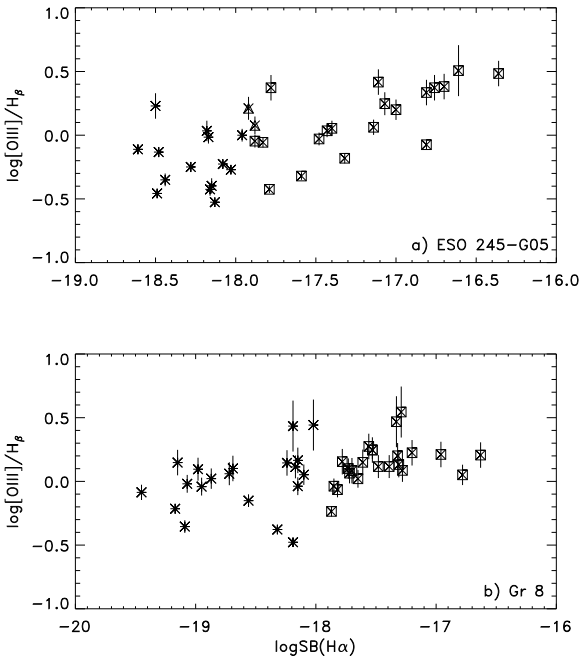

Fig. 3.— The log SB(Hα) vs. [OIII]/Hβ for Gr 8 (panel b) and ESO 245-G05 (panel a). Symbols as in Figure 4. There is a clear correlation for the H II regions of ESO 245-G05 that become flatter for the DIG locations. The correlation is less step for Gr 8 with no abrupt change in the slope between DIG and H II regions.

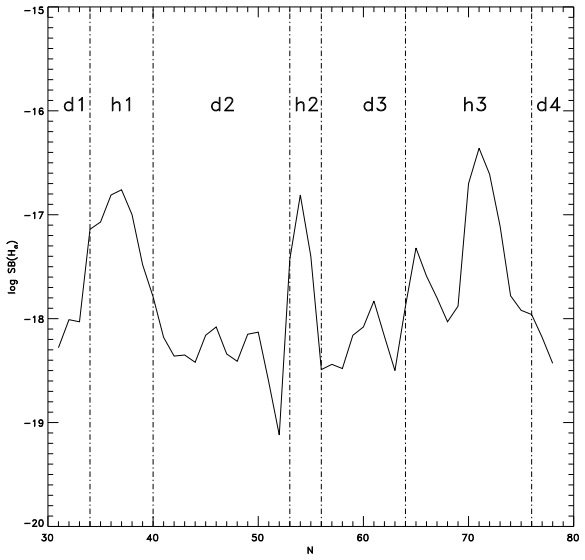

Fig. 4.— The surface brightness along the slit position in ESO 245-G05. The H II regions, marked with their names, are located inside the dashed-dotted lines. Spectrum nr 52 is one of the data points which value is below the noise level.

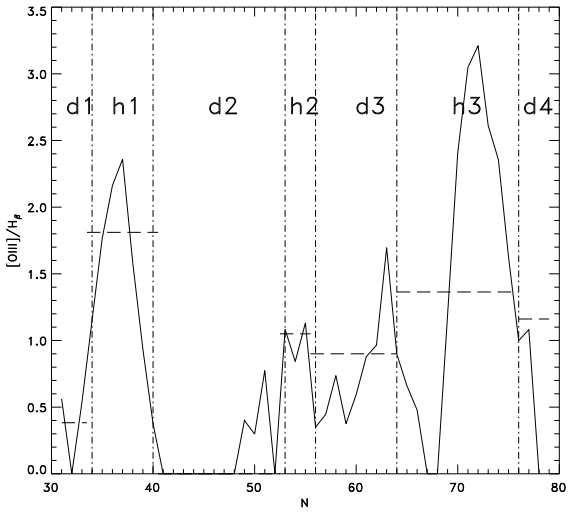

Fig. 5.— The [OIII]/Hβ along the slit position in ESO 245-G05. The H II regions are located inside the dashed-dotted lines. The long-dashed lines correspond to the values from the integrated spectra. The largest excitation corresponds to the second condensation of *h3*

.

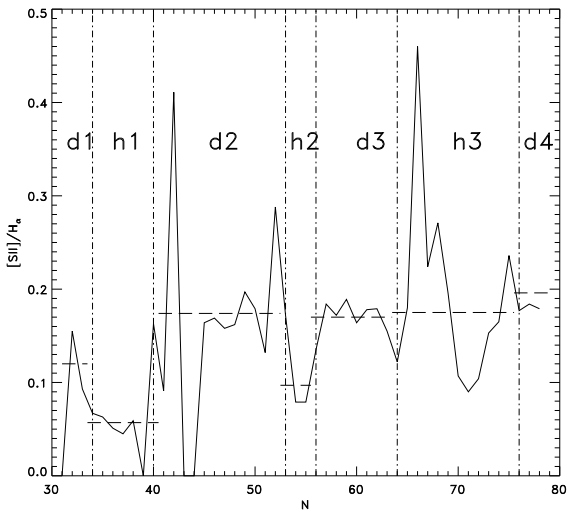

Fig. 6.— The [SII]/Hα ratio along the slit position in ESO 245-G05. Symbols as in Fig. 5. It is very remarkable the large value of this ratio inside *h3* (see text for details).

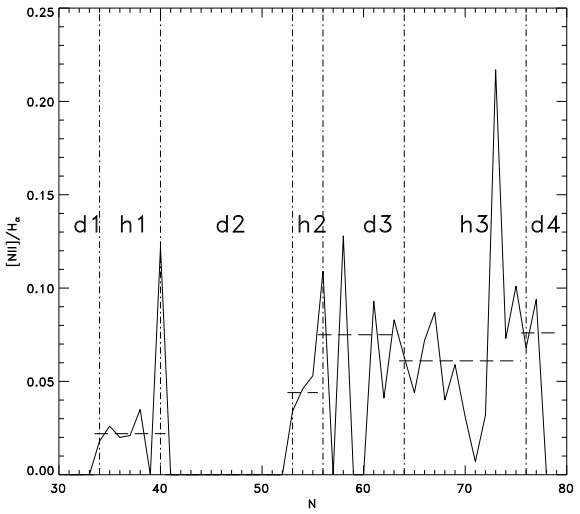

Fig. 7.— The [NII]/Hα ratio along the slit in ESO 245-G05. Symbols as in Fig. 5. Again, *h3* has the largest value of this ratio. On the contrary, nitrogen is no detected in any place of *d2* but one.

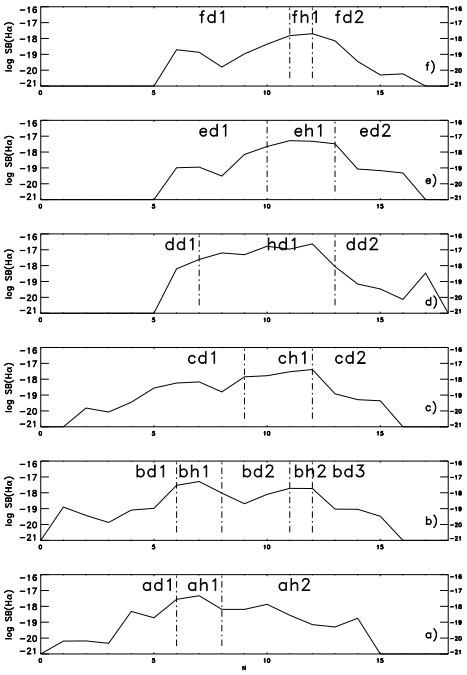

Fig. 8.— Plot of the SB(Hα) along the slits in Gr 8. Slit *f* corresponds to the northen part of the galaxy and slit *a* to the southern. There is a migration of the H II regions from the west (left in the figure) to the east of the galaxy.

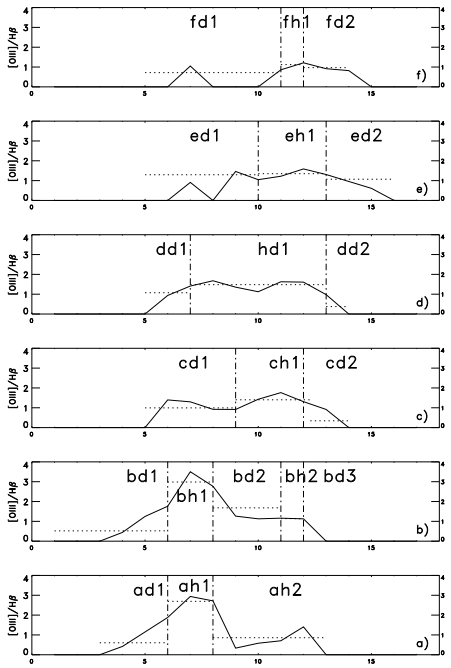

Fig. 9.— The [OIII]/Hβ along the slits in Gr 8. In addition to the lines in Fig. 8, the dotted lines correspond to the value of the integrated spectra. The largest [OIII]/Hβ is located at the south part of the galaxy (region No 5 in Hodge et al. 1989), decreasing towards the north. The migration of the [OIII]/Hβ to the east is also very prominent.

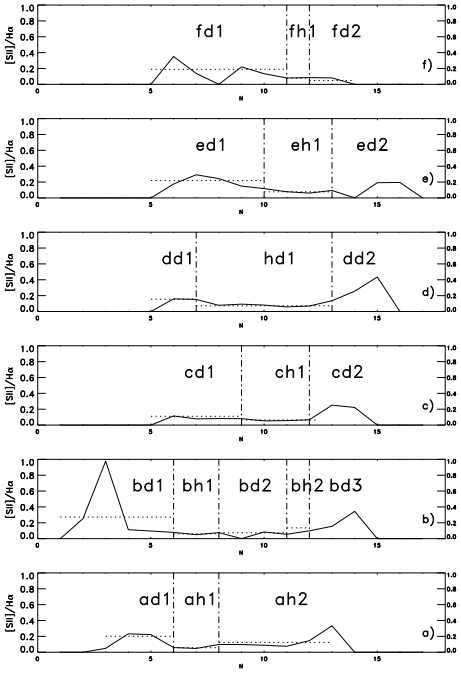

Fig. 10.— The [SII]/Hα ratio along the slits in Gr 8. Symbols as in Fig. 9. Except for the spectrum nr 3 in *bd1* and nr 15 in *dd2*, the rest of the values are smaller than 0.3, indicating the absence of shocks.

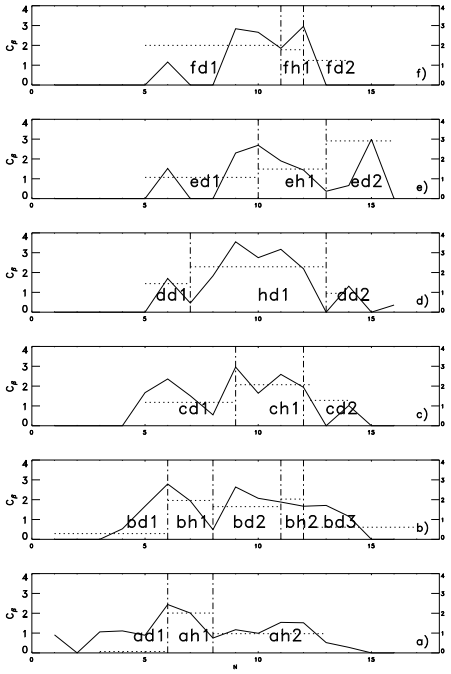

Fig. 11.— The extinction coefficient along the slits in Gr 8. Symbols as in Fig. 9. We see that the extinction is not homogeneous inside the galaxy, as concluded from the studies in H I. The Galactic extinction towards this galaxy corresponds to a C_β = 0.04.

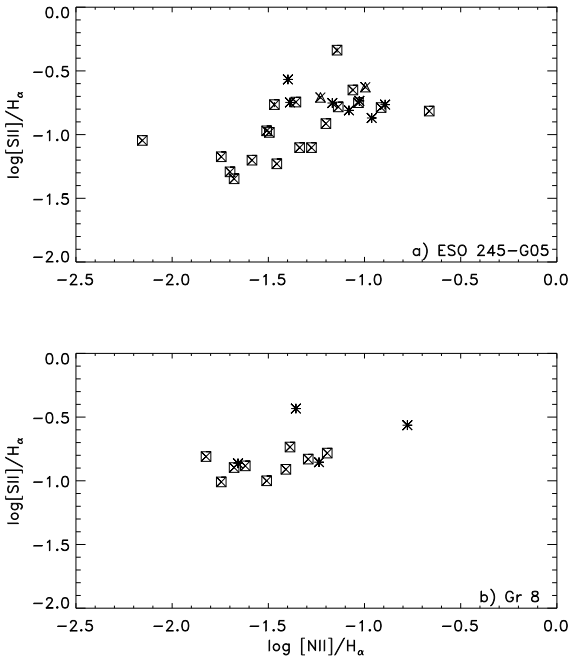

Fig. 12.— The diagnostic diagram log[SII]/Hα vs. log[NII]/Hα for ESO 245-G05 (panel a) and Gr 8 (panel b). Stars correspond to DIG locations and squares to H II regions. All the data points from the r-spectra with their uncertainty are presented in this plot. A strong correlation is observed between these two parameters at the DIG in spiral galaxies. Such a correlation is not presented here but a trend.

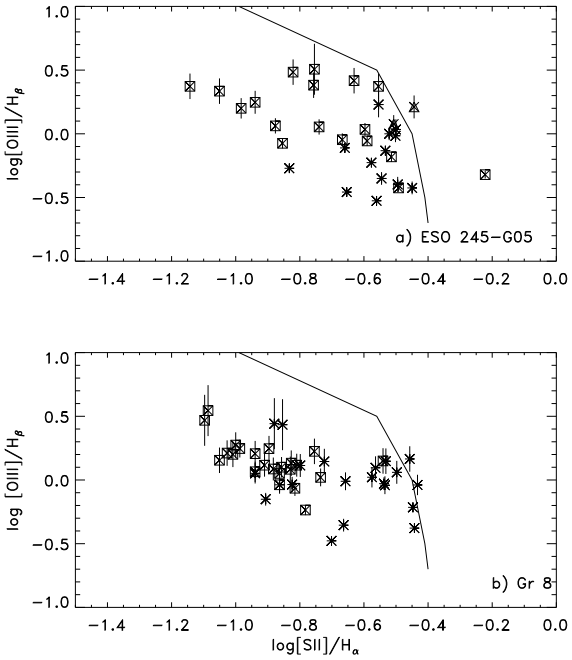

Fig. 13.— The diagnostic diagram log[OIII]/Hβ vs. log[SII]/Hα. Symbols as in figure 12. The line divides the diagram into the photoionized region (to the left) and the shocked one (to the right). Except for one H II of ESO 245-G05, the rest of the locations lie in the photoionized region.

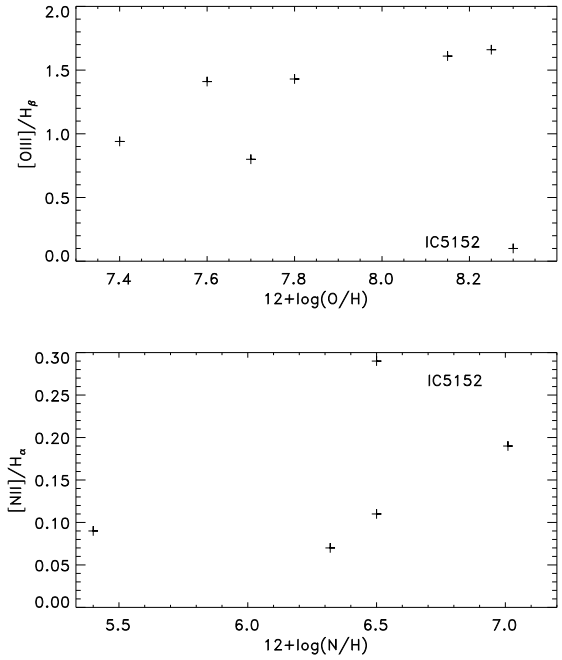

Fig. 14.— The relation between the [OIII]/Hβ of the DIG and the oxygen content of the ISM (panel a) and the ratio [NII]/Hα and the nitrogen abundance (panel b) for a sample of irregular galaxies. No real correlation is found between them. In both panels the oddest galaxy is IC 5152.

Table 1: The log of the observations. The slit positions observed are presented in column 1. Column 2 shows the date of observation while the seeing is given in column 3 in arcsecond. The total integration time is presented in column 4 and the air mass in column 5. Column 6 gives the telescope coordinates for ESO 245-G05 and the reference slit position of Gr 8 while the rest of the positions is given by the number of arcseconds the telescope drifted from the initial position.

Position	Date	Seeing	Int. Time	Air Mas.	Comments
ESO 245-G05 No 12	090897	1.2"	$90^m/60^m$	1.08/1.04	$01^h45^m05^s$ -43°37′21"
Gr 8 slit a	140302	2.0"	30^m	1.07	$12^h58^m47^s$ 14°12′15"
Gr 8 slit b	140302	2.0"	30^m	1.05	4" to the North
Gr 8 slit c	140302	1.5"	30^m	1.12	10" to the North
Gr 8 slit d	140302	1.5 "	105^m	1.3	13" to the North
Gr 8 slit e	130302	1.8"	60^m	1.4	15" to the North
Gr 8 slit f	130302	1.8"	45^m	1.2	19" to the North

Table 2: The uncertainties in the lines observed for every slit position for the spectral lines studied. The name of the slit is presented in column 1, while the uncertainty, in percentage, is given in the other columns. The uncertainty in the nitrogen line is based on very few measurements for each slit.

Position	[OIII]λ5007	Hα	[NII]λ6583	[SII]λ6717	[SII]λ6731
ESO 245-G05	27 %	18 %	78 %	56 %	55 %
Gr 8 slit a	7 %	14 %	10 %	29 %	23 %
Gr 8 slit b	8 %	11 %	33 %	18 %	18 %
Gr 8 slit c	12 %	11 %	8 %	50 %	25 %
Gr 8 slit d	7 %	47 %	52 %	14 %	30 %
Gr 8 slit e	7 %	23 %	19 %	30 %	12 %
Gr 8 slit f	8 %	11 %	-	11 %	11 %

Table 3: Line ratios (non-extinction corrected) of the integrated spectra for ESO 245-G05. Column 1 identifies the location along the slit. H refers to H II region and d to DIG locations. The last column corresponds to the S/N in the recombination line Hα.

Location	[OII]/Hβ	[OIII]/Hβ	[NII]/Hα	[SII]6717 Å/Hα	[SII]λ6717/[SII]λ6731	S/N(Hα)
d1	1.94±0.05	0.38±0.01	-	0.12±0.01	3.2 ±0.3	5.7
h1	2.36±0.01	1.811±0.002	0.022 ±0.001	0.057±0.002	1.24±0.04	93
d2	3.19±0.03	-	0.076±0.002	0.174±0.006	1.1±0.2	12
h2	2.281±0.007	1.05±0.001	0.044±0.001	0.097±0.007	1.4±0.1	125
d3	4.1±0.1	0.90±0.01	0.075±0.004	0.170±0.007	1.61±0.07	10
h3	3.36±0.02	1.364±0.003	0.061±0.005	0.175±0.003	1.49±0.01	90
d4	6.23±0.03	1.16±0.001	0.08±0.01	0.196±0.004	1.57±0.06	12

Table 4: Line ratios of integrated spectra for Gr 8. Column 1 identifies the slit position with the letter from Table 1. H refers to H II regions and d to DIG locations. When more than one is at the same slit, a number is given. The [OIII]/Hβ is shown in column 2 while the [NII]/Hα is presented in column 3, when detected. Column 4 gives the HeI/Hβ for the few H II regions where it was detected and column 5 the [SII]/Hα. Finally, the extinction coefficient in the recombination line Hα is shown in column 6 and the S/N in Hα in column 7.

Location	[OIII]λ5007Å/Hβ	[NII]λ6584Å/Hα	He I (λ5876 Å)/Hβ	[SII]λ6717 Å/Hα	C$_\beta$	S/N(Hα)
ad1	0.603±0.06	-	-	0.201±0.02	0.11±0.006	5
ah1	2.693±0.1	-	-	0.057±0.004	2.05±0.1	28
ad2	0.859±0.05	-	-	0.124±0.007	1.01±0.05	7
bd1	0.520±0.03	-	-	0.272±0.02	0.33±0.02	5
bh1	2.983±0.1	0.016±0.001	0.031±0.002	0.061±0.004	2.00±0.1	27
bd2	1.681±0.1	-	-	0.074±0.01	1.69±0.1	10
bh2	1.138±0.08	-	-	0.074±0.005	2.07±0.1	15
bd3	-	-	-	0.136±0.01	0.65±0.1	5
cd1	0.995±0.09	-	-	0.111±0.01	1.22±0.06	2
ch1	1.402±0.07	0.022±0.002	0.022±0.002	0.064±0.004	2.11±0.1	32
cd2	0.342±0.04	-	-	-	1.32±0.1	6
dd1	1.073±0.06	-	-	0.155±0.01	1.47±0.1	4
dh1	1.481±0.07	-	0.012±0.0007	0.072±0.004	2.33±0.1	15
dd2	0.375±0.02	-	-	-	0.99±0.05	14
ed1	1.296±0.1	-	-	0.219±0.02	1.11±0.07	5
eh1	1.350±0.08	0.020±0.002	0.008±0.001	0.077±0.005	1.53±0.09	20
ed2	-	0.092±0.01	-	-	2.95±0.1	-
fd1	0.719±0.1	-	-	0.190±0.03	2.04±0.2	2
fh1	1.122±0.06	0.030±0.002	-	0.078±0.005	1.82±0.09	14

Table 5: Photon leakage (in %) and ionization temperatures for the integrated spectra for Gr 8 based on the line ratios. Columns 2 and 3 correspond to the data from the excitation and columns 4 and 5 are based on the [SII]/Hα ratio. In two cases, *cd1* and *dd1* only two values are possible.

Location	Leakage [OIII] (%)	T_{ion} K	Leakage [SII](%)	T_{ion}
ad1	58 %	38,000	30-45 %	40,000-30,000
ad2	53 %	38,000	30-40 %	36,000-30,000
bd1	75 %	38,000	40-80 %	38,000
bd2	30-80 %	47,000-38,000	30-35 %	34,000-30,000
bd3	-	-	30-40 %	36-30,000
cd1	50 or 80 %	38,000 or 41,000	30-38	38,000-30,000
cd2	55 %	35,000	-	-
dd1	50 or 80 %	38,000 or 41,000	30-40	38,000-30,000
dd2	55 %	35,000	-	-
ed1	40-80 %	38,000-44,000	35-50 %	40,000-30,000
ed2	-	-	-	-
fd1	60 %	38,000	30-45 %	40,000-30,000